






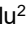



## Synthesis of $(Cr,V)_x C_y$ -T MXene Materials from $(Cr,V)_2 AlC$ MAX Phase Produced via Powder Metallurgy Methods

Semih Ateş<sup>1</sup> , İlayda Süzer<sup>2</sup> , Ahmet Mirza Erol<sup>2</sup> , Ahmed Emin Tok<sup>2</sup> , Berkay Demircan<sup>2</sup> , Hüseyin Kerim Yazıcı<sup>2</sup> ,  
C. Fahir Arısoy<sup>1</sup> , M. Lütfi Öveçoğlu<sup>2</sup> , Duygu Ağaoğulları<sup>2</sup> 

<sup>1</sup>Istanbul Technical University, Faculty of Chemical & Metallurgical Engineering, Metallurgical and Materials Eng. Dep., 34469, Istanbul, Türkiye.

<sup>2</sup>Istanbul Technical University, Faculty of Chemical & Metallurgical Engineering, Metallurgical and Materials Eng. Dep., Particulate Materials Laboratories (PML), Graphene & 2D Materials Laboratory, 34469, Istanbul, Türkiye.

**Abstract:** MAX ( $M_{n+1}AX_n$ ) phases represent a class of ternary metallic ceramics distinguished by their remarkable properties, rendering them highly sought after across various applications. Among these, their role as precursors for the production of 2D MXene materials stands out prominently in the realm of advanced ceramics. MXenes are obtained through the selective etching of the A-element layers from MAX phases, resulting in ultrathin layers with unique characteristics. The predominant method for MXene synthesis involves wet chemical processes, typically employing HF etching. These layered structures exhibit exceptionally high surface areas, positioning them as frontrunners for electronic applications. In this study,  $(Cr,V)_2 AlC$  precursor was produced by pressureless sintering of mechanically milled pure metallic powder mixtures. Subsequently, the MAX phase precursor was subjected to HF etching to obtain  $(Cr,V)$ -C-based MXenes. Both MAX and MXenes were analysed with XRD, SEM-EDS methods, and micro-hardness measurements. According to the results, the Optimal morphology which revealed a layered MXene structure for wet chemical etching of produced MAX phase materials was obtained after 4 hours of high-energy ball-milled Cr, V, Al, and C starting powder mixtures. Furthermore, the surface terminations (-T) which are an inevitable consequence of the regular chemical etching process, were identified following the analysis of the etched MXenes. In conclusion, this study accentuates the importance of optimizing synthesis methods for MAX phases to obtain tailored MXene materials, crucial for advancing applications in advanced ceramics.

**Keywords:** MAX, MXene, powder metallurgy.

## $(Cr,V)_2 AlC$ MAX Fazından Toz Metalurjisi Yöntemleriyle $(Cr,V)_x C_y$ -T MXene Malzemelerinin Üretimi

**Özet:** MAX ( $M_{n+1}AX_n$ ) fazları, üstün mekanik ve termal özellikleri ile ileri teknoloji seramik malzemeler içerisinde yer alan malzeme grubudur. Uygulama alanları arasında kaplamalar yer alsa da yeni nesil iki boyutlu MXene malzemelerin üretimi için de üretim başlangıcı fazlar olarak kullanılmaktadır. MXen malzemeler, MAX fazında yer alan A-elementi katmanlarının selektif (seçici) olarak çözündürülmesi ile elde edilmektedir. Böylece, elde edilen nihai MXene malzemeler birçok ince katmandan oluşmaktadır ve MAX fazı ile aynı hacim içerisinde çok yüksek yüzey alanı oluşturmaktadır. MXene üretimi için sıklıkla MAX fazının HF ile çözümlendirilmesini içeren yaş kimyasal yöntemler kullanılmaktadır. Elde edilen ince ve çok katmanlı yapının sağladığı yüksek yüzey alanı, MXene malzemelerin elektronik uygulamalarda üstün özellikler sergilemesini sağlamaktadır. Bu çalışmada, mekanik olarak öğütülmüş saf metalik toz karışımlarının basınçsız sinterleme yöntemi ile  $(Cr,V)$  – C temelli MXene malzemelerinin eldesi için HF çözümlendirme yöntemi uygulanmıştır. MXene üretiminin başlangıç malzemesi olan MAX fazı üretimi için Cr, V, Al ve C metalik tozlarına yüksek enerjili bilyalı öğütücüde farklı öğütme süreleri uygulanmıştır. Öğütülen toz karışımı pelet haline getirilmiş ve basınçsız olarak inert atmosferde sinterlenmiştir. Elde edilen  $(Cr,V)_2 AlC$  MAX fazı ve bu fazın HF ile çözümlendirilmesi ile üretilen MXene malzemelerine XRD, SEM-EDS ve mikrosertlik analizleri uygulanmıştır. Elde edilen sonuçlara göre, yaş kimyasallar yöntemlerle elde edilmesi hedeflenen katmanlı MXene malzemesi için optimum morfolojiye sahip MAX fazı 4 saat öğütme süresi ile sağlandığı tespit edilmiştir. Ayrıca, yaş kimyasal yöntemler ile selektif olarak çözümlendirmenin bir sonucu olan yüzey bileşikleri (-T), elde edilen MXene malzemelerde de tespit edilmiştir. Sonuç olarak bu çalışmada, ileri teknoloji seramik malzemelerden olan yeni nesil 2-boyutlu yapılar için MAX fazı üretim sürecinin optimizasyonunda ilk adım olan öğütme süreci ve MAX fazı morfolojisinin sonuç malzemesi özelliklerine etkileri incelenmiştir.

**Anahtar Kelimeler:** MAX, MXene, toz metalurjisi.

### Article

**Corresponding Author:** C. Fahir Arısoy<sup>1</sup>, Duygu Ağaoğulları<sup>2</sup>, E-mail: fahir@itu.edu.tr<sup>1</sup>, bozkurtd@itu.edu.tr<sup>2</sup>

**Reference:** Ateş, S., Süzer, İ., Erol, A. M., Tok, A. E., Demircan, B., Yazıcı, H. K., Arısoy, C. F., Öveçoğlu, M. L., & Ağaoğulları, D. (2024), Synthesis of  $(Cr,V)_x C_y$ -T MXene materials from  $(Cr,V)_2 AlC$  MAX phase produced via powder metallurgy methods, *ITU Journal of Metallurgy and Materials Engineering*, 1(1) 16–21.

Submission Date : 29 April 2024

Online Acceptance : 24 July 2024

Online Publishing : 26 July 2024

## 1. Introduction

MAX phase materials, combine the properties of metals and ceramics to constitute a fascinating area of advanced ceramic materials. They are characterized by their peculiar formula of  $M_{n+1}AX_n$ , where M is an early transition metal, A is an A-group element, and X is either carbon or nitrogen. They are the perfect choice for a wide range of cutting-edge applications thanks to their extraordinary combination of qualities, which include high-temperature stability, good mechanical strength, and oxidation resistance.

The M-X bonds within MAX phase materials are characterised by exceptional strength, owing to the coexistence of covalent and metallic bonding mechanisms. Conversely, M-A bonds exhibit relatively weaker interactions, which contribute to the formation of a layered structure. This unique combination of covalent and metallic characteristics provides a distinctive category which is the intersection of metallics and ceramics (Biswas et al., 2021).

The Cr-V-Al-C MAX phase stands out within this material family due to its exceptional properties that render it highly suitable for a wide array of applications. The sintering temperature is relatively lower than those of other MAX phases such as TiAlC which is a widely studied type [1]. Also, solid solution formation provides more out-of-ordinary characteristics (Völker et al., 2021; Zhang et al., 2021). While MAX phases have applications in mechanical engineering, they are most frequently employed as precursor materials for the top-down production of MXenes in contemporary research.

MXene materials are two-dimensional (2D) materials. MXene accepts a variety of hydrophilic terminations, and its surface can be terminated by functional groups such as O, F, OH, and Cl. MXene materials exhibit unique physical and chemical properties, such as metal conductivity, hydrophilicity, high ion migration, large specific surface area, and easy surface modification. These properties make MXene materials versatile for various applications, including catalysis, batteries, energy conservation, and biomedicine. The development of MXene materials has been undergoing exponential growth and has the potential to revolutionize various industries (G. Ali et al., 2021; I. Ali et al., 2022; Gogotsi & Anasori, 2019; Kedambaimoole et al., 2022; Qin et al., 2021).

The production of MXenes can be categorized into two main methodologies: bottom-up and top-down. In the top-down approach, individual sheets are obtained through the chemical or mechanical exfoliation of bulk crystals (Martins et al., 2020). The process of generating MXenes involves the separation of 2D layers from MAX phases, akin to the behaviour of graphite, albeit with stronger interlayer bonds than those found in graphite flakes. Consequently, the assumption derived from graphite exfoliation does not hold for MAX phases. While MAX phase materials lend themselves to exfoliation, the pioneering production of MXenes was achieved through the chemical exfoliation of aluminum in  $Ti_3AlC_2$  using HF-etching (Zhou et al., 2021). Mechanical exfoliation has historically posed challenges due to the robustness of the ductile metallic bonds in MAX phases, although it has been successfully applied to large single-crystal MAX materials (Gkountaras et al., 2020). Chemical etching relies on the formation of covalently bonded layers through the reaction of molecular blocks. The choice of etchant is intricately linked to the intrinsic chemistry of the "A" element and the pre-existing A-A and M-A bonds within the MAX phases. Additionally, the etchant medium plays the primary role in determining the intended application field. For

instance, when  $Ti_3Al_2C_2$  is etched in a  $LiF_2$  solution, it yields  $Ti_3C_2F_x$  and  $Li^+$  solution, making it suitable for battery applications, resulting in  $Ti_3C_2$  with surface terminations ("T") of  $F_x$ . The presence of HF moieties during this process facilitates the separation of interlayers. The F/H termination of HF molecules contributes to the weakening of Al-Ti bonds, as HF molecules progressively intercalate into the MAX phase. This intercalation results in the formation of  $AlF_3$  as an interlayer gap, enabling further HF molecule intercalation. Additionally,  $H_2O$  participates in the reaction by terminating the MXene with the -OH group (Xu et al., 2021).

MAX phase materials are typically synthesized through the sintering of a homogenous mixture of metallic forms of starting powders and carbon. The sintering process can be achieved using advanced techniques such as spark plasma sintering (SPS), as well as simpler methods like pressureless sintering. Subsequently, the sintered products are subjected to etching processes to obtain MXenes (Abdolhosseinzadeh et al., 2021; Fundamental Aspects and Perspectives of MXenes | SpringerLink, n.d.; MAX Phases and MXenes Synthesis, 2022).

In this study, Cr-V-Al-C MAX phase materials were synthesized by mixing metallic Cr, V, and Al powders and carbon at different mechanical milling durations, followed by sintering at  $1400^\circ C$ . This allowed for an investigation into the impact of the mechanical alloying duration on the resulting phases. Furthermore, starting powder mixtures were prepared with the ratio of 1:1:1 with  $Cr=V$  and  $Cr>V$  proportions to examine their effects on the stoichiometry of the final product. Subsequently, Cr-V-C MXene material was obtained through the conventional hydrofluoric acid (HF) etching method. The synthesized MAX and MXene materials were analyzed using X-ray diffraction (XRD) and scanning electron microscopy (SEM) coupled with energy-dispersive X-ray spectroscopy (EDS). Furthermore, microhardness measurements were implemented in both produced MAX and MXene materials.

## 2. Materials and Methods

### 2.1 Materials

The properties of starting materials for the production of MAX phase precursors are given in Table 1.

Table 1. The properties of starting powder materials.

Tablo 1. Başlangıç malzemelerinin özellikleri.

Material	Purity (%)	Particle size ( $\mu m$ )
Cr	99,99	74
V	99,9	44
Al	99,9	40-44
Graphite	99,99	<20

The high-energy ball milling was implemented with stainless steel vials and containers. After the obtain of pellets from milled powders HF was used for selective etching. The solution was prepared according to 1M.

### 2.2 Methods

The starting powder mixture was prepared from elemental Cr, V, Al, and graphite powders by high-energy ball milling (SPEX™ Mixer Mill 8000D) for 1 and 4 h. After ball milling, powders were cold isostatic pressed (under 200 tons) to obtain green bodies. After that, pressureless sintering was implemented to pellets under Ar gas flow (8 L/min) at  $1400^\circ C$  for 4 h. In-furnace natural cooling was applied for 24h. After sintering the MAX phases were observed using XRD (Bruker™ D8 Advance) and SEM-EDS (Thermofischer and Hitachi TM-1000) techniques.

MXenes were produced from pressureless sintered MAX phases with HF etching method. Unlike to literature, the sintered pellets were not crushed to generate clearly visible MXene layers. The etching was implemented at room temperature for 30 days in an HF solution. The MXenes were analyzed by XRD and SEM-EDS methods.

### 3. Results and Discussion

The XRD results of 1 and 4 h milled different powder mixtures which were produced according to Cr:V:Al:C = 0.5:0.5:1:1 and 0.75:0.25:1:1 stoichiometric ratios, are given in Figure 1. According to XRD results, the mechanical alloying was avoided which provides unchanged stoichiometry. Because, if mechanical alloying occurs, it changes the stoichiometry of the mixture and results in undesired alloyed and carbide phases after sintering. Also, as a result of the high energy provided with high ball milling duration, the grain sizes of the final mixture were decreased which resulted in wider and more noisy peaks.

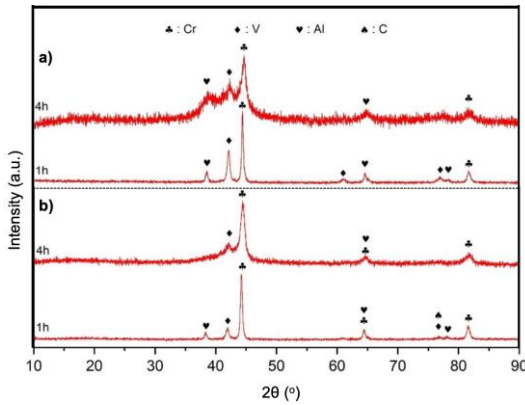


Figure 1. XRD result of 1 and 4 h milled powder mixtures according to Cr:V:Al:C = 0.5:0.5:1:1 (a) and 0.75:0.25:1:1 (b) stoichiometric ratios.

Şekil 1. Cr:V:Al:C = 0,5:0,5:1:1 (a) ve 0,75:0,25:1:1 (b) stokiyo metrilere göre 1 ve 4 saat öğütme uygulanmış toz karışımlarının XRD sonuçları.

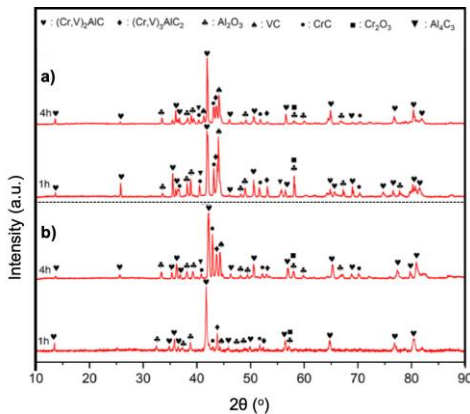


Figure 2. XRD results of sintered pelleted powders which were milled for 1 and 4 h and mixed according to Cr:V:Al:C = 0.5:0.5:1:1 (a) and 0.75:0.25:1:1 (b) stoichiometric ratios.

Şekil 2. Cr:V:Al:C = 0,5:0,5:1:1 (a) ve 0,75:0,25:1:1 (b) stokiyo metrilere göre 1 ve 4 saat öğütme uygulanmış toz karışımlarının peletleme ve sinterleme sonrası XRD sonuçları.

A representative SEM-EDS result of sintered pellets that were prepared by 1 and 4 h ball-milling of mixtures is given in Figure 3. The representative SEM imaging method was implemented because the stoichiometry of powder mixtures had slight differences which did not result in any chemical composition impact. It was observed that the sintered materials contained pores and segregations. Especially on EDS mapping, dark regions have Cr, V, and C, and white regions contain Al. High matrix formation was observed for 4 h milled powders. This was linked with lower particle sizes which were provided with higher ball-milling duration.

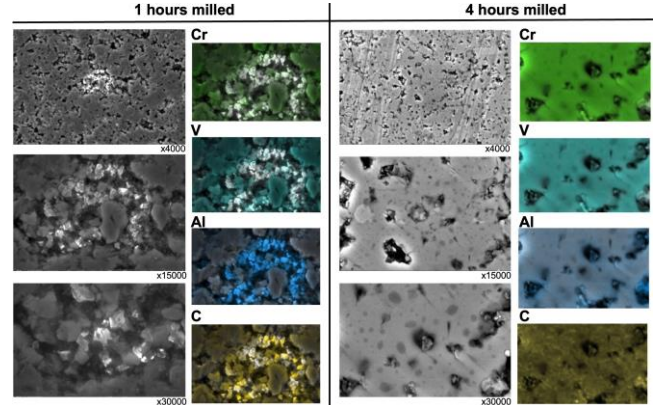


Figure 3. Representative SEM and EDS mapping results after sintering 1 and 4 h milled powders.

Şekil 3. 1 ve 4 saatlik öğütülmüş tozların sinterlenmesinden sonra temsili SEM ve EDS haritalama sonuçları.

Point EDS results are given in Figure 4. EDS results show that the sample contains all elements in each region. According to atomic ratios, the chemical compositions of each stoichiometry were calculated and the results were in Table 2. In accordance with the stoichiometric ratio of  $M_{n+1}AX_n$ , it has been observed that there are different phases within the calculated chemical compositions, and this examination corresponded with the XRD results (Figure 2). If MAX phases were taken as  $M_{n+1}AX_n$  chemical formulation, the 1 h milled powders and point 1 of 4 h milled powders did not show appropriate MAX compositions. The matrix that was observed for 4 h milled powders was also examined with area EDS results and showed Cr:0.75, V:0.3, Al:0.3, C:0.3. Thus, aimed Cr:V ratio (Cr:V = 0.75:0.25) was obtained but Al and C were segregated.

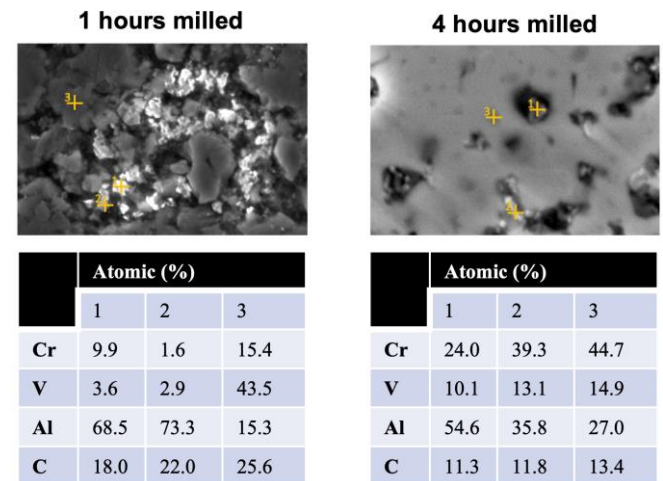


Figure 4. Point EDS results.  
Şekil 4. Noktasal EDS sonuçları.

Table 2. Calculated compositions according to point EDS results and resulted in MAX phase chemical formula.  
 Tablo 2. Noktasal EDS sonuçlarına göre hesaplanan bileşimler ve ilgili MAX fazı kimyasal formülleri.

	1-h milled	MAX phase chemical formula	4-h milled	MAX phase chemical formula
Point 1	Cr <sub>0.31</sub> V <sub>0.11</sub> Al <sub>2.14</sub> C <sub>0.56</sub>	M <sub>0.4</sub> A <sub>2.1</sub> X <sub>0.5</sub>	Cr <sub>0.75</sub> V <sub>0.32</sub> Al <sub>1.7</sub> C <sub>0.35</sub>	M <sub>1</sub> A <sub>1.7</sub> X <sub>0.4</sub>
Point 2	Cr <sub>0.05</sub> V <sub>0.1</sub> Al <sub>2.3</sub> C <sub>0.7</sub>	M <sub>0.1</sub> A <sub>2.3</sub> X <sub>0.7</sub>	Cr <sub>1.2</sub> V <sub>0.4</sub> Al <sub>1.1</sub> C <sub>0.4</sub>	M <sub>1.6</sub> A <sub>1.1</sub> X <sub>0.4</sub>
Point 3	Cr <sub>0.5</sub> V <sub>1.4</sub> Al <sub>0.5</sub> C <sub>0.8</sub>	M <sub>0.6</sub> A <sub>0.5</sub> X <sub>0.8</sub>	Cr <sub>1.4</sub> V <sub>0.5</sub> Al <sub>0.8</sub> C <sub>0.4</sub>	M <sub>1.9</sub> A <sub>0.8</sub> X <sub>0.4</sub>

The micro-Vickers hardness measurement results of sintered 4 h milled Cr:V:Al:C = 0.5:0.5:1:1 and 0.75:0.25:1:1 powders are given in Table 3. The hardness values were found as quite close to each other. However, the deviation showed that Cr>V stoichiometry had lower hardness variation.

Table 3. Micro-Vickers hardness measurement results of sintered 4h milled powders.

Tablo 3. 4 saat öğütülmüş ve sinterlenmiş MAX fazlarının mikrosertlik ölçüm sonuçları.

Composition of starting powder mixture	Average Hardness (GPa)	Standard Deviation
0.5:0.5:1:1	4.7	1.98
0.72:0.25:1:1	4.4	1.10

After the observation of 4 h milling showed optimal morphology for etching to produce MXene material, the 4 h milled Cr:V:Al:C = 0.5:0.5:1:1 and 0.75:0.25:1:1 powders etched with HF. The XRD results of etched samples are given in Figure 5. After etching the XRD results of samples showed H-F-O bonded compositions which were formed due to etchant. These were the higher surface termination amounts. To generate a clear surface, grinding was implemented to an etched pellet with a 2000 grid size sand-paper for 1 min at 110 rpm. Even though these peaks were not observed after grinding, it can be assumed that very limited surface termination could remain on the structure, which was related to literature studies.

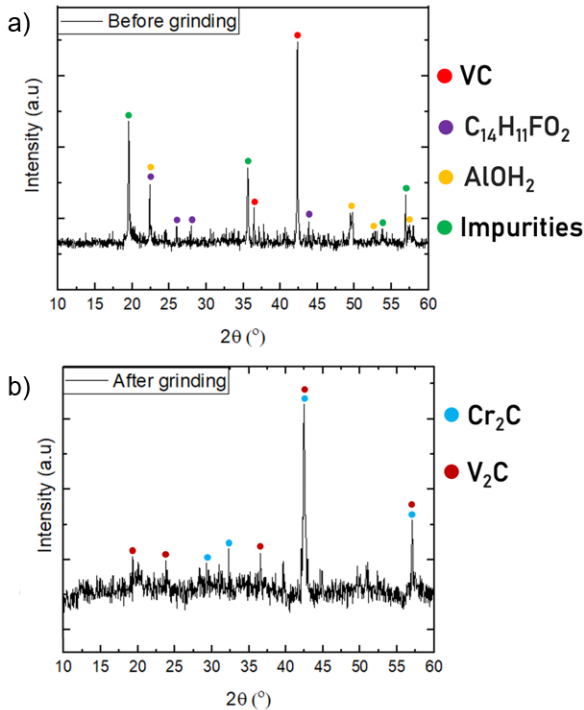


Figure 5. XRD results of etched MAX phase material before (a) and after grinding (b): MXene material.

Şekil 5. MAX fazının selektif olarak çözümlendirilmesiyle elde edilmesi MXenelerin a) Zımparalama öncesi, b) Zımparalama sonrası XRD sonuçları.

The XRD results of the produced MXene material, which provide an in-depth interpretation of the crystal structure and solid solution, are presented in Figure 6. Ibrahim et. al. (2022) observed impurities effects on crystal structure parameters and computed that lattice parameters and interplanar spacing could vary in between 2.96-3.19Å and 2.09-2.20Å, respectively. Also, Champagne et. al. (2018) observed the crystal structure of V<sub>2</sub>C as  $P\bar{3}m1$  space group. In the presented study Cell Search was conducted according to XRD pattern (see Figure 6) via the Treor90 method (Suzuki et al., 2020; Werner, 1964). Table 4 shows calculated crystal structure information. According to calculated results the crystal structure was found as P6<sub>3</sub>/mmc with 6,77 Å (a), 6,77 Å (b), 20.6 Å (c) and 90° (α), 90° (β), 120° (θ). Kanoun et. al. (2012) revealed that all ternary MXene materials, M<sub>n+1</sub>AX<sub>n</sub> (n = 1, 2, or 3), belongs to P6<sub>3</sub>/mmc crystal structure that was related with produced MXene material. Also, Salim et. al. (2019) reported that all MXenes should be in hexagonal closed-packed (HCP) systems. Despite M<sub>2</sub>X being favored to exhibit HCP, M<sub>3</sub>X<sub>2</sub> and M<sub>4</sub>X<sub>3</sub> are aligned with a face-centered cubic (FCC) structure. The P6<sub>3</sub>/mmc is related with β-V<sub>2</sub>C (Chong et al., 2014). Also, Cr<sub>2</sub>C showed P6<sub>3</sub>/mmc crystal structure with lowest formation energy as similar to V<sub>2</sub>C. The formation energies of Cr<sub>2</sub>C and V<sub>2</sub>C P6<sub>3</sub>/mmc were -0.409 eV and -1.452 eV, respectively (Abderrahim et al., 2012).

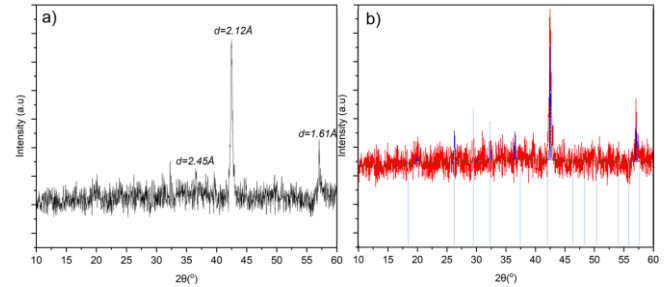


Figure 6. a) Examined XRD pattern of produced MXene, b) referenced XRD pattern of P6<sub>3</sub>/mmc crystal structure with blue line on MXene XRD pattern with red line.

Şekil 6. a) Üretilmiş MXene'nin incelenen XRD sonucu, b) kırmızı çizgi ile belirtilmiş MXene XRD deseni üzerinde mavi çizgi ile belirtilmiş referans P6<sub>3</sub>/mmc kristal yapısına ait XRD deseni.

Table 4. Calculated crystal structure parameters.  
 Tablo 4. Hesaplanmış kristal yapı parametreleri.

2θ (°)	Interplanar spacing (Å)	h/k/l
36	2.45	1/1/6
42	2.12	1/0/9
57	1.61	2/2/4

The SEM results of etched and ground samples are given in Figure 6. EDS results are given in Table 4. The results showed layered structures. Approximately, each layer was distanced at 800 nm. Also, a very highly porous medium was examined in general which hindered the micro-Vickers hardness measurement. According to EDS-area results, the Al was found as in residual ratios. Also, Cl showed a shred of evidence for surface terminations, and some impurities were observed in the XRD pattern before grinding.

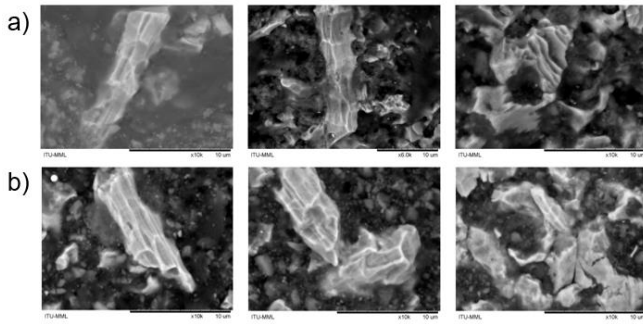


Figure 7. SEM images of MXene particles produced with etching of MAX phases according to Cr:V:Al:C = a) 0.5:0.5:1:1 and b) 0.75:0.25:1:1 starting powder mixture stoichiometry.

Şekil 7. Cr:V:Al:C = a) 0,5:0,5:1:1 ve b) 0,75:0,25:1:1 başlangıç tozu karışımı stokiyometrisine göre MAX fazlarının selektif olarak çözümlenirilmesi ile üretilen MXene partiküllerinin SEM görüntüleri.

Table 5. Area EDS results of SEM images of related particles. Tablo 5. SEM görüntüleri verilen partiküllerin bölgesel EDS sonuçları.

Element	Region 1 (wt.%)		Region 2 (wt.%)		Region 3 (wt.%)	
	(a)	(b)	(a)	(b)	(a)	(b)
Al	2.1	2.8	5.4	5.8	6.2	8.0
Cr	68.3	69.3	67.8	68.0	70.9	70.0
V	15.2	9.7	19.2	18.2	21.8	22.0
C	2.3	0.3	1.2	1.5	1.1	0.5
Impurities	12	12.5	6.5	6.5	3.1	0.5

The layered appearance of the layered structure was due to the hexagonal crystal structure described in the previous section, where selectively leached Al forms metallic atoms filling the hexagonal structure and carbon atoms were located in orthogonal planes. As a result, differentiation in the elemental distribution of the structure is inherent in the MXene materials appearance. The absence of the layered structure inherent in MXene materials implies heterogeneous elemental distribution. Therefore, the high Cr content and low V content indicate that the aimed Cr = V ratio was not achieved in MXene production. On the other hand, considering that the solid solution state does not change the crystal structure, the near-perfect matching of the XRD pattern with a single crystal structure and the detection of heterogeneity in the elemental distribution analysis indicate that the material could contain a high amount of solid solution MXene with discrete Cr<sub>2</sub>C and V<sub>2</sub>C phases.

#### 4. Conclusion

The synthesis of MAX and MXene materials involved a meticulously controlled process beginning with the preparation of starting powder mixtures containing elemental Cr, V, Al, and graphite, subjected to ball-milling for 1 and 4 h. Subsequent pressureless sintering was conducted on the pellets under an Ar atmosphere at 1400°C. The sintered 4 h milled powders predominantly exhibited (Cr,V)<sub>2</sub>AlC phases, with aluminum and chromium oxide. Additionally, the impact of ball-milling duration on phase intensity and the formation of VC and Cr<sub>3</sub>C<sub>7</sub> phases were evident. SEM-EDS analysis revealed compositional variations within the sintered materials, especially notable matrix formation was observed for 4 h milled and sintered pellets. Ultimately, this investigation found that 4 h milling produced an optimal morphology for etching to produce MXene materials according to the dispersed matrix morphology. MXene materials, with subsequent etching, yielded H-F-O bonded compositions on the surface. Grinding

was employed to achieve a clear surface, minimizing remaining surface terminations. The layered structure of MXene material was clearly visible in the SEM images.

#### 5. Acknowledgements

We would like to thank Res. Assist. Mertcan Kaba and Prof. Dr. Hüseyin Çimenoglu for SEM-EDS analysis of MXene materials and Dr. Doğa Bilican and Assist. Prof. Dr. Nuri Solak for SEM-EDS analysis of MAX phase materials.

#### 6. Conflicts of Interest

The authors declare no conflict of interest.

#### 7. References

- Abderrahim, F. Z., Faraoun, H. I., & Ouahrani, T. (2012). Structure, bonding and stability of semi-carbides M<sub>2</sub>C and sub-carbides M<sub>4</sub>C (M=V, Cr, Nb, Mo, Ta, W): A first-principles investigation. *Physica B: Condensed Matter*, 407(18), 3833-3838. <https://doi.org/10.1016/j.physb.2012.05.070>
- Abdolhosseinzadeh, S., Jiang, X., Zhang, H., Qiu, J., & Zhang, C. (John). (2021). Perspectives on solution processing of two-dimensional MXenes. *Materials Today*, 48, 214-240. <https://doi.org/10.1016/j.mattod.2021.02.010>
- Ali, G., Iqbal, M. Z., & Iftikhar, F. J. (2021). MXene. In *Advances in Supercapacitor and Supercapattery* (pp. 255-269). Elsevier. <https://doi.org/10.1016/B978-0-12-819897-1.00005-7>
- Ali, I., Faraz Ud Din, M., & Gu, Z.-G. (2022). MXenes Thin Films: From Fabrication to Their Applications. *Molecules*, 27(15), 4925. <https://doi.org/10.3390/molecules27154925>
- Biswas, A., Natu, V., & Puthirath, A. B. (2021). Thin-film growth of MAX phases as functional materials. *Oxford Open Materials Science*, 1(1), itab020. <https://doi.org/10.1093/oxfmat/itab020>
- Champagne, A., Shi, L., Ouisse, T., Hackens, B., & Charlier, J.-C. (2018). Electronic and vibrational properties of V<sub>2</sub>C-based MXenes: From experiments to first-principles modeling. *Physical Review B*, 97(11), 115439. <https://doi.org/10.1103/PhysRevB.97.115439>
- Chong, X., Jiang, Y., Zhou, R., & Feng, J. (2014). Electronic structures mechanical and thermal properties of V-C binary compounds. *RSC Adv.*, 4(85), 44959-44971. <https://doi.org/10.1039/C4RA07543A>
- Khalid, M., Grace, A. N., Arulraj, A., & Numan, A. (Eds.). (2022). *Fundamental aspects and perspectives of MXenes*. Springer.
- Gkoutaras, A., Kim, Y., Coraux, J., Bouchiat, V., Lisi, S., Barsoum, M. W., & Ouisse, T. (2020). Mechanical Exfoliation of Select MAX Phases and Mo<sub>4</sub>Ce<sub>4</sub>Al<sub>7</sub>C<sub>3</sub> Single Crystals to Produce MXenes. *Small*, 16(4), 1905784. <https://doi.org/10.1002/sml.201905784>
- Gogotsi, Y., & Anasori, B. (2019). The Rise of MXenes. *ACS Nano*, 13(8), 8491-8494. <https://doi.org/10.1021/acsnano.9b06394>
- Ibrahim, I. A. M., Abdel-Azeim, S., El-Nahas, A. M., Kühn, O., Chung, C.-Y., El-Zatahry, A., & Shibli, M. F. (2022). In Silico Band-Gap Engineering of Cr<sub>2</sub>C MXenes as Efficient Photocatalysts for Water-Splitting Reactions. *The Journal of Physical Chemistry C*, 126(35), 14886-14896. <https://doi.org/10.1021/acs.jpcc.2c03622>

- Kanoun, M. B., Goumri-Said, S., & Abdullah, K. (2012). 8— Theoretical study of physical properties and oxygen incorporation effect in nanolaminated ternary carbides 211-MAX phases. İçinde I. M. Low (Ed.), *Advances in Science and Technology of Mn<sup>+</sup>1AX<sub>n</sub> Phases* (pp. 177-196). Woodhead Publishing. <https://doi.org/10.1533/9780857096012.177>
- Kedambaimoole, V., Harsh, K., Rajanna, K., Sen, P., Nayak, M. M., & Kumar, S. (2022). MXene wearables: Properties, fabrication strategies, sensing mechanism and applications. *Materials Advances*, 3(9), 3784-3808. <https://doi.org/10.1039/D1MA01170G>
- Martins, V. L., Neves, H. R., Monje, I. E., Leite, M. M., Oliveira, P. F. M. D., Antoniassi, R. M., Chauque, S., Morais, W. G., Melo, E. C., Obana, T. T., Souza, B. L., & Torresi, R. M. (2020). An Overview on the Development of Electrochemical Capacitors and Batteries – Part I. *Anais Da Academia Brasileira de Ciências*, 92. <https://doi.org/10.1590/0001-3765202020200796>
- MAX Phases and MXenes Synthesis. (2022, Nisan 15). A.J. Drexel Nanomaterials Institute. <https://nano.materials.drexel.edu/max-phases-and-mxenes-synthesis/>
- Qin, R., Shan, G., Hu, M., & Huang, W. (2021). Two-dimensional transition metal carbides and/or nitrides (MXenes) and their applications in sensors. *Materials Today Physics*, 21, 100527. <https://doi.org/10.1016/j.mtphys.2021.100527>
- Salim, O., Mahmoud, K. A., Pant, K. K., & Joshi, R. K. (2019). Introduction to MXenes: Synthesis and characteristics. *Materials Today Chemistry*, 14, 100191. <https://doi.org/10.1016/j.mtchem.2019.08.010>
- Suzuki, Y., Hino, H., Hawai, T., Saito, K., Kotsugi, M., & Ono, K. (2020). Symmetry prediction and knowledge discovery from X-ray diffraction patterns using an interpretable machine learning approach. *Scientific Reports*, 10(1), 21790. <https://doi.org/10.1038/s41598-020-77474-4>
- Völker, B., Stelzer, B., Mráz, S., Rueß, H., Sahu, R., Kirchlechner, C., Dehm, G., & Schneider, J. M. (2021). On the fracture behavior of Cr<sub>2</sub>AlC coatings. *Materials & Design*, 206, 109757. <https://doi.org/10.1016/j.matdes.2021.109757>
- Werner, P.-E. (1964). Trial-and-error computer methods for the indexing of unknown powder patterns. *Zeitschrift für Kristallographie - Crystalline Materials*, 120(1-6), 375-387. <https://doi.org/10.1524/zkri.1964.120.16.375>
- Xu, J., Peng, T., Qin, X., Zhang, Q., Liu, T., Dai, W., Chen, B., Yu, H., & Shi, S. (2021). Recent advances in 2D MXenes: Preparation, intercalation and applications in flexible devices. *Journal of Materials Chemistry A*, 9(25), 14147-14171. <https://doi.org/10.1039/D1TA03070A>
- Zhang, Z., Duan, X., Jia, D., Zhou, Y., & van der Zwaag, S. (2021). On the formation mechanisms and properties of MAX phases: A review. *Journal of the European Ceramic Society*, 41(7), 3851-3878. <https://doi.org/10.1016/j.jeurceramsoc.2021.02.002>
- Zhou, A., Liu, Y., Li, S., Wang, X., Ying, G., Xia, Q., & Zhang, P. (2021). From structural ceramics to 2D materials with multi-applications: A review on the development from MAX phases to MXenes. *Journal of Advanced Ceramics*, 10(6), 1194-1242. <https://doi.org/10.1007/s40145-021-0535-5>